DERIVATION/VALIDATION OF COLLISION CROSS SECTIONS FOR IONS AND ELECTRONS IN GASES FROM MEASURED SWARM COEFFICIENTS

J. DE URQUIJO

Instituto de Ciencias Físicas, Universidad Nacional Autónoma de México, P.O. Box 48-3, 62251, Cuernavaca, Mor., México
jdu@fis.unam.mx

ABSTRACT

This paper presents a few selected cases of recent experimental work on the measurement of transport and reaction properties of electron and ion swarms in gases and their usefulness to either validate or derive sets of collision cross sections which are essential for the understanding, simulation and modelling of many types of gas discharges. The paper discusses several key examples of measured electron/ion drift velocities (mobilities), longitudinal diffusion coefficients, effective ionization coefficients, and ion-molecule reaction rates with gases through which new sets of cross sections have been obtained. All the systems discussed contemplate the measurement of the pure gas and its mixture with N_2 or rare gases for which reliable cross section sets are well known, thereby serving as a test to the newly derived cross sections for the pure gas.

1. INTRODUCTION

Electron and ion interactions with gases at low energies have been studied for several decades. Essentially, two kinds of experiments exist, namely single collision, beam experiments, aimed at measuring cross sections, and multicollisional swarm experiments from which macroscopic, coefficients are normally obtained. Both cross sections and swarm coefficients are related to each other [1], and in many cases measured swarm coefficients are used to either derive or validate cross section sets.

Nowadays there is an increasing need for either electron and ion swarm transport and reaction coefficients or the respective cross sections in view of the ever growing low temperature plasma applications and basic research on atmospheric physics, for instance. The swarm technique has been very helpful in providing a wealth of data for many gases and mixtures, and in particular the pulsed Townsend technique, based on the observation of the temporal development of the discharge from which several transport and reaction data are derived. Swarm techniques have so far provided transport coefficients such as electron and ion drift velocities, diffusion coefficients and/or reaction coefficients such as electron impact ionization and attachment. Only in comparatively few cases electron detachment coefficients and reaction rates have been derived. The reason for this stems from the fact that modelling the Townsend avalanche is difficult since it involves the solution of coupled continuity equations for the charge carrier species involved in the process, hence this has only been possible for relatively simple cases such as electron/ion drift, ionization and attachment. Even simple cases such as electron detachment have been successfully solved for the electron component of the discharge, the ion part remaining unsolved thoroughly because of its analytical complexity. Thus, the need to solve the set of continuity equations numerically, taking into account the special boundary and initial conditions is called for [2].

2. ELECTRONS

Our discussion starts with the selection of three successful examples of validation of cross section sets from measured swarm coefficients for electrons.

2.1 R134a

There is an increasing interest among the plasma modelling community for electron transport and collision data for 1,1,1,2 tetrafluoroethane, also known as R134a, HFCR134a or $C_2H_2F_4$. This gas is currently used extensively as a coolant and in many other gas discharge applications such as chemical vapour deposition, nanostructure growth and plasma etching. R134a is also used in

radiation particle detectors and resistive plate chambers. Despite the strong need for reliable swarm and cross section data, there are only two swarm measurements [3,4] the latter covering a wider range of E/N both for the pure gas and its mixture with Ar. The work of Sasic et al [5] represents a careful effort to derive a self consistent cross section set for $C_2H_2F_4$, validated with the calculation of the same set of swarm parameters for the $C_2H_2F_4$-Ar mixture, relying on the already proven and highly reliable cross section set for Ar.

A preliminary set of cross sections [6] was employed using firstly a two-term Boltzmann equation solver (TT), followed by an accurate Monte Carlo calculation (MC). A standard swarm analysis of measured drift velocities and effective ionization coefficients for pure $C_2H_2F_4$ was performed (Fig. 1), and the results were presented in its preliminary form in [7]. Applying the same technique to the gaseous mixture improves the uniqueness of the cross sections, thereby making it possible to extend the energy range and shift the sensitivity from momentum transfer to energy transfer cross sections [8-11]. Both initial and improved cross section sets are plotted in Fig. 1.

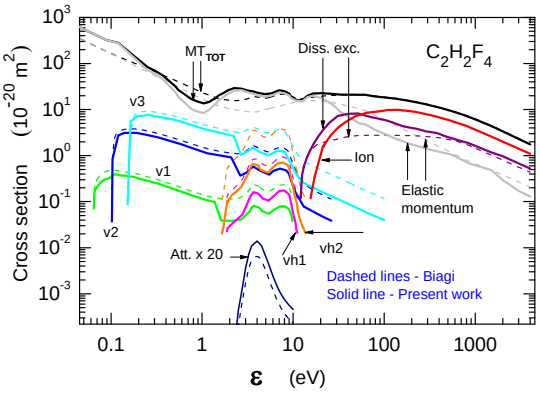

Figure 1. *Cross section set for electron interactions $C_2H_2F_4$ as a function of energy [5]. The dashed lines represent the initial cross section set of Biaggi [6]. The solid lines represent the results derived from measured swarm data. v_1, v_2 and v_3 denote vibrational excitation at low energies whereas vh_1, vh_2 and vh_3 correspond to higher energies. MT_{TOT}: total momentum transfer; Diss. exc: dissociative excitation; Ion: ionization, Att: attachment.*

To illustrate the fitting procedure, Figs. 2 and 3 display measured and calculated electron drift velocities in $C_2H_2F_4$ and $C_2H_2F_4$-Ar, both with the Two-Term and Monte Carlo methods, there being very good agreement between them after optimisation of the cross section set, whereas the original cross section set provides only a poor fit to the swarm data.

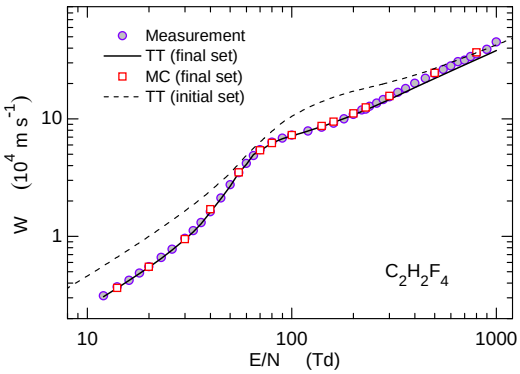

Figure 2. *The electron drift velocities W in pure $C_2H_2F_4$. The present MC calculated data (final set) are compared with the calculated data of the initial set [6] and with measurements [7].*

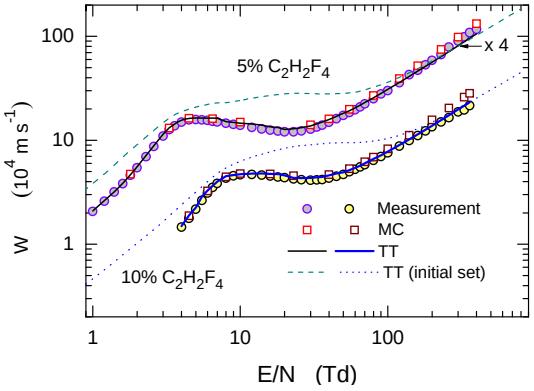

Figure 3. *Drift velocities W for electrons in mixtures with 5% and 10% $C_2H_2F_4$ in Ar [7]. Measured and calculated values for the 5% mixture have been multiplied by a factor of 4 to avoid overlap of the two sets of curves.*

The calculated and measured values of the effective ionisation coefficient $(\alpha-\eta)/N$ (α and η are the ionisation and attachment coefficients, respectively) in $C_2H_2F_4$ are shown in Fig. 4, where one can see again a very good agreement between measured and calculated coefficients with the improved cross section set.

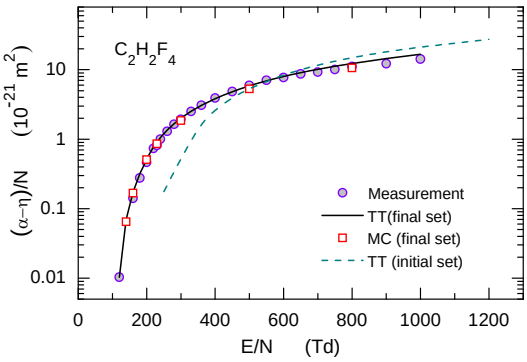

Figure 4. *Effective ionization coefficients for electrons in pure $C_2H_2F_4$ [7]. The TT and MC data calculated with the improved cross section set are compared with those calculated with the initial one. [6].*

Finally, an example of the density-normalised longitudinal diffusion coefficients ND_L is given in Fig. 5. While the agreement between calculation and measurement is good for E/N>100 Td, it becomes poor below this value. This difference is ascribed to the difficulties of assessing reliable D_L data from the pulsed Townsend experiment at low E/N since the gas pressure has to be raised, thereby impairing the observation of the fall of the pulse, which is convoluted with the time response of the associated instrumentation [12].

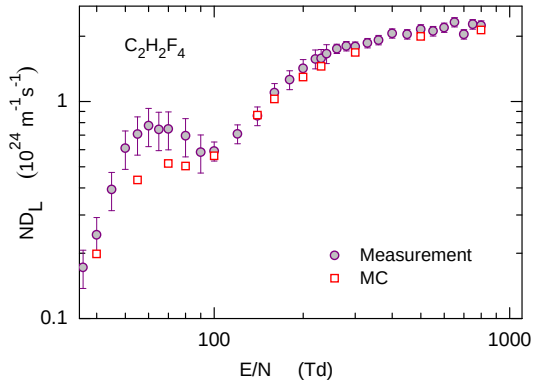

Figure 5. *The density-normalized longitudinal diffusion coefficients for electrons in $C_2H_2F_4$. Measurements were taken from [7] and the Monte Carlo (MC) calculations were made with the final set of cross sections [5,7].*

2.2 H_2O

Water vapour, one of the most important molecules, has been studied scarcely in comparison with other gases such as SF_6 [13]. The reason for this stems partially from the fact that its relatively low saturation vapour pressure (~20 Torr at room temperature) makes it difficult to cover wide ranges of E/N. On the other hand, water forms clusters readily, both positive and negatively charged.

The most recent calculation of the electron drift velocity in water vapour [14] is shown in Figure 6, where one can see good agreement between theory and experiment up to E/N=300 Td, above which value the only two measured sets of data depart, a fact that has been explained theoretically in terms of two different approximations, namely bulk and flux, corresponding to the use of double shutter drift tubes and pulsed Townsend apparatus, respectively.

The measured data of Ref. [17] were also tested successfully for the mixtures of H_2O with N_2, O_2 and CO_2, using a different cross section set [19], an example of which is given in Fig. 7 for the electron drift velocity in H_2O-N_2 mixtures.

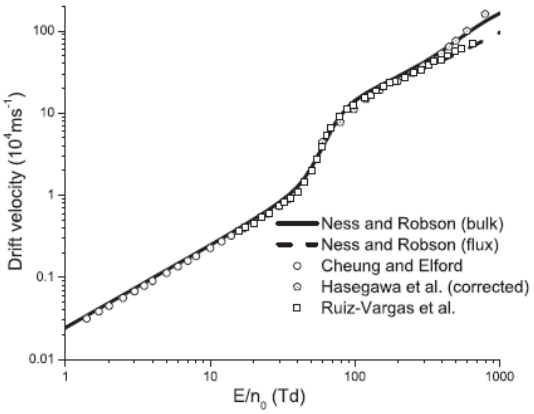

Figure 6. *Measured electron drift velocities in water vapour from Cheung and Elford [15], Hasegawa et al [16]and Ruiz-Vargas et al [17]), and calculated by Ness and Robson [18].*

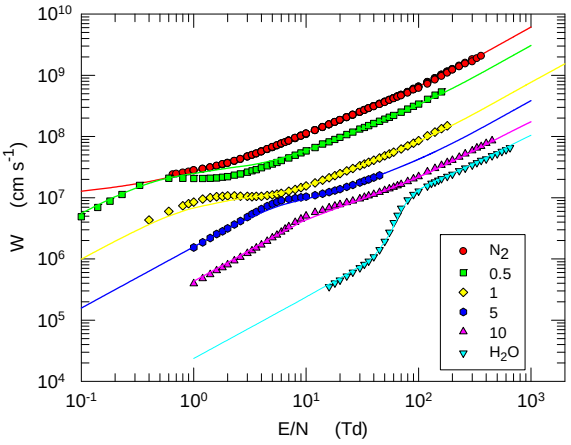

Figure 7. *Electron drift velocity in H_2O-N_2 mixtures [17]. Symbols are the measurements and the solid lines are the calculations.*

2.3 N_2O

N_2O is another gas of interest in view of its relevance to atmospheric processes. A procedure similar to that described above for $C_2H_2F_4$ was followed to improve the cross section set for N_2O. The original cross section set was assembled from several sources [20], and is given in Fig. 8, together with the improved set [20]. Note in Fig. 8 that the attachment cross section kept its shape while its absolute value changed after the fitting procedure.

A good example of the improvement of the cross section set for electrons in N_2O is that given in Fig. 9 for the electron drift velocity in the mixtures of N_2O with N_2, measured with a

pulsed Townsend apparatus and calculated from a Two-Term approximation.

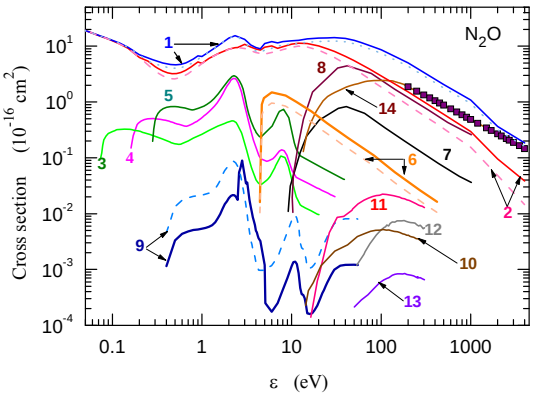

Figure 8. *Improved cross section set (solid lines) and original (broken lines) as a function of electron energy for N_2O [20]. Total momentum transfer (1), elastic momentum transfer (2), vibrational excitation (3-5), electronic excitation (6-8), dissociative attachment (9), dissociative electronic excitation (10–13), ionization (14, including the squares).*

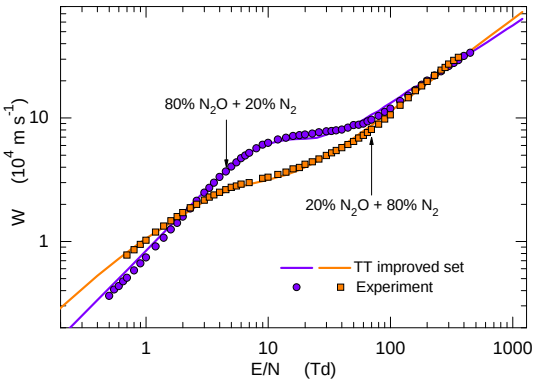

Figure 9. *Electron drift velocities in N_2O-N_2 mixtures. Symbols are measured values [20] and lines are Two-Term (TT) calculations using the improved cross section set in Fig. 8 [20].*

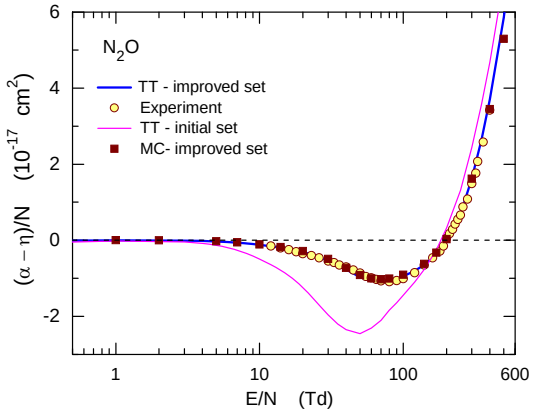

Figure 10. *Effective ionisation coefficients in N_2O calculated by the Two-Term (TT) and Monte Carlo (MC) methods and measurements. Taken from Ref. 20.*

A further test of the consistency of the cross section set for electron interactions with N_2O is that observed in Fig. 10 for the variation of the effective ionisation coefficient $(\alpha-\eta)/N$ in N_2O as a function of E/N, where the substantial difference between the values calculated with the initial and improved cross section sets for E/N<100 Td is evident.

3. IONS

In spite of the importance of ions in many types of discharges comparatively little is yet known about their transport and reactivity in the gas. Negative ions, for instance, may be a source of extra electrons in the realm of the discharge arising from electron detachment, or positive ions may do their part through Penning ionisation, and also both ionic species interacting with the walls, to name only a few. These processes are frequently ignored more by the null or scarce knowledge about them than by their relative insignificance. In the absence of more information, it is common to realise that modellers resort to simple transport and reaction formulas that are only crude approximations. One of the reasons for this is that measuring and calculating transport properties of ions is far more difficult than for electrons. This section discusses four successful examples of derivation/validation of ion collision cross sections.

3.1 Mixtures of Xe with Ne and He

Rare gases are widely used nowadays in a large number of gas discharge devices. For instance, mixtures of Xe with Ne and/or He are used in plasma display panels and low-pressure gas discharge lamps developed for mercury-free vacuum ultraviolet sources and fluorescent lamps or lasers. An important issue with these applications is a knowledge of the ion mobilities in order to determine their mean energies in the discharge since these are influential in the ion-molecule reactions and surface material interactions [21].

The first attempt to measure the mobility of Xe^+ in the mixture of Xe and Ne was with a double mass spectrometer drift tube. These measurements turned out to be troublesome and inaccurate for two main reasons: (a) the low pressure regime (<0.1 Torr) to work with because of the presence of the mass spectrometers, and (b) the different effusion rates of Xe, Ne and He through the entrance and exit

orifices of the drift tube that caused the original mixture composition to change inside the drift region. Notwithstanding the lack of mass spectrometry in their Pulsed Townsend apparatus, the authors of Ref. [22] were able to demonstrate that the predominant drifting ion was Xe^+ in contrast with Ne^+ and He^+, both formed by electron impact and also charge transfer from Xe^+. Once the limits and conditions of the experiment were well established, these authors were able to measure the mobility of Xe^+ in the Xe-Ne and Xe-He mixtures over a wide range of E/N. Previously calculated density-normalised mobilities, μN, using a previous set of cross sections [21], were found in good agreement as seen in Figs. 11 and 12 for the Xe-Ne and Xe-He mixtures, respectively.

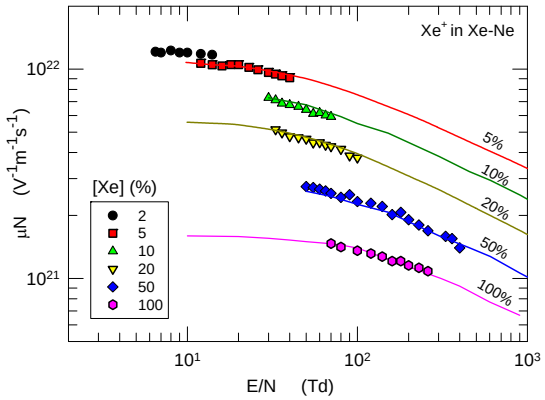

Figure 11. *The density-normalised mobility, μN, of Xe^+ in Xe-Ne mixtures. Symbols are measured values [22] and solid lines are calculations using a cross section set given in Ref. [21].*

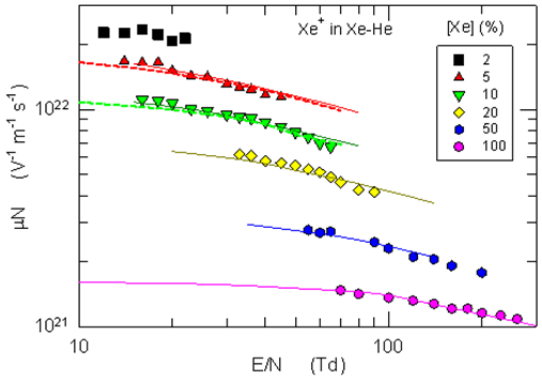

Figure 12. *The density-normalised mobility, μN, Xe^+ in Xe-He mixtures. Symbols are measured values [22] and solid lines are calculations with a cross section set given in Ref. [21].*

3.2 N_2O

Transport properties of negative ions in N_2O are scarce in spite of the influence of this gas in the atmosphere under discharge conditions. Measurements of negative ions from a pulsed Townsend experiment were carefully analysed. After a thorough bibliographical revision it was concluded that the majority ion formed in the Townsend discharge was $N_2O_2^-$ [23]. These mobilities are shown in Fig. 13. The procedure used evaluate the mobility was to firstly determine the cross sections using the momentum transfer theory [23] as the initial step to fit the experimental results and obtain the energy dependence of these cross sections. Final adjustments were made in order to achieve the best possible agreement with the measurements. The detachment cross sections were calculated and considered in the simulation, as shown in Fig. 14 for collisions of $N_2O_2^-$ with N_2O and N_2. Again, in order to obtain a unique cross section set the calculations were done for both N_2O and N_2O-N_2.

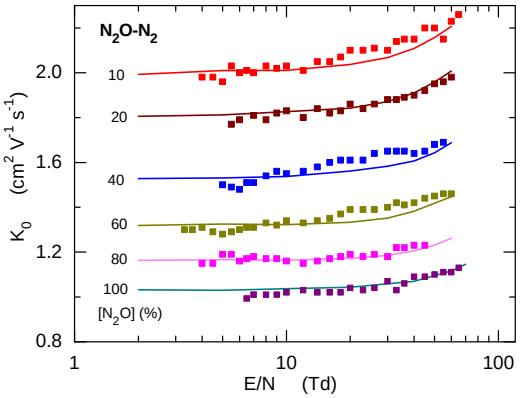

Figure 13. *Reduced mobility K_0 of $N_2O_2^-$ in N_2O and its mixtures with N_2 [23]. Symbols are measurements and the solid lines are the calculations.*

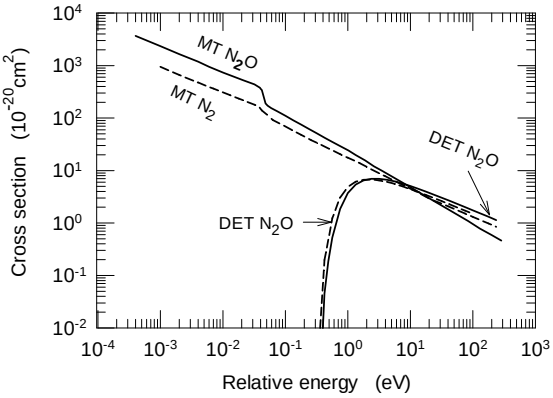

Figure 14. *Momentum transfer and detachment cross sections for $N_2O_2^-$ colliding with N_2O and N_2 [23].*

3.3 Negative ions of SF_6

SF_6 is an insulating gas of great importance for the electrical industry in spite of its high global

warming potential. Efforts to dilute this gas with other, much less harmful gases to the environment have been made, aiming at keeping most of the outstanding properties of the pure gas. SF_6 is one of the most electronegative gases known, forming negative ions readily under discharge conditions. Here we shall discuss the derivation of collision cross sections of SF_6^- in the SF_6 mixture with O_2. A drawback of these calculations was the lack of information on inelastic cross sections of SF_6^- with O_2, leading the authors to use those for Ne, which were the only available.

Figure 15 shows the measured [24] and calculated reduced mobilities, K_0, for the SF_6-O_2 mixtures. The mobility of SF_6^- was calculated for the gas mixtures from an optimized Monte Carlo code for the ion transport simulation in a drift tube. The elastic momentum transfer collision cross sections were determined from a semi-classical JWKB approximation using a 12-4 interaction potential, while those due to inelastic collisions (detachment, dissociative charge transfer and SF_6^- conversion to SF_5^- and F^-) were taken from the literature and are shown in Fig. 16 [24].

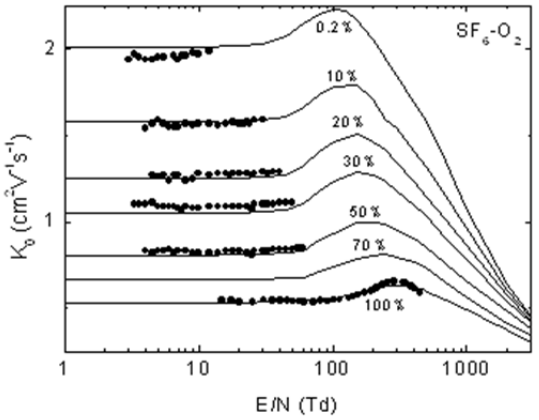

Figure 15. *Reduced mobility data, K_0, of $SF6^-$ in SF_6-O_2 mixtures for several SF_6 concentrations [24]; symbols: measurements; solid lines: calculations.*

The combination measurement-calculation provides more insightful results than the independent provision of cross sections and swarm transport data. Moreover, knowledge and derivation of cross section sets from measured data over a restricted range of E/N enables the calculation over extended ranges, as is evident for the SF_6-O_2 mixture.

Figure 17 shows a calculation of the distribution function derived from this study for the SF_6^- species moving in Ne, SF_6 and the 50-50% SF_6-Ne mixture. Here, one clearly sees how the ion reaches much higher energies in Ne than in SF_6 or its mixture with Ne.

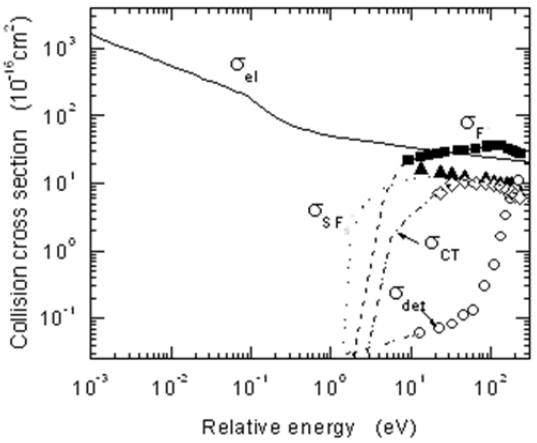

Figure 16. *Collision cross section set for the SF_6^-/SF_6 system. σ_{el}: elastic; $\sigma(F^-)$: ion conversion to F-; $\sigma(SF_5^-)$: ion conversion to SF_5^-; σ_{CT}: charge transfer; σ_{det}: electron detachment form SF_6^-. The broken lines represent the extrapolations of the inelastic cross sections at lower energies [24].*

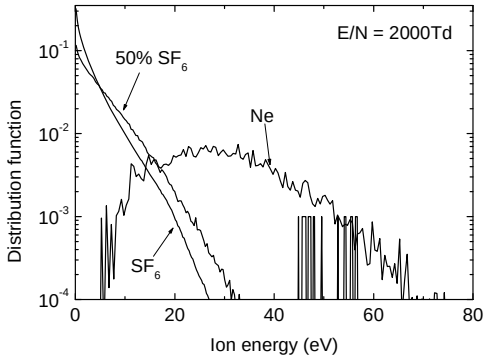

Figure 17. *Energy distribution function of SF_6^- in SF_6, Ne and in the SF_6-Ne (50:50) mixture For (a) E/N= 10 Td and (b) E/N=2000 Td. From Ref. 24.*

3.4 Negative ions in O_2

Well defined negative ion signals from a pulsed Townsend experiment in O_2 suggested the presence of two distinct ionic species drifting and reacting as the negative ion clouds moved across the discharge gap. Previous knowledge of O_4^- formation from O_2^-, the latter formed by electron impact, led to propose a reaction scheme leading to the formation of the ionic clusters O_4^- and O_6^- through three body reactions [25]. A very representative signal of this process is given in Fig. 18, showing the temporal evolution of both

ionic components, calculated from a pulsed Townsend avalanche simulator [2].

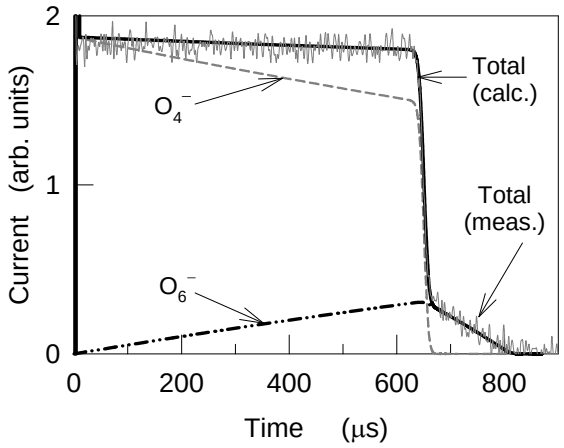

Figure 18. *Measured negative ion transient in oxygen at E/N=8 Td, gas pressure of 598.5 Torr, and drift distance of 3.1 cm [25], clearly displaying the presence of two different drifting and reacting species in the discharge gap.*

Further insight into the fast formation of O_4^- is given by the avalanche simulation of Fig. 19, showing how O_2^- is converted into O_4^- during the first few 100 ns of discharge development, as compared with the ionic drift times of O_4^- and O_6^- in the hundreds of μs regime (Fig. 18).

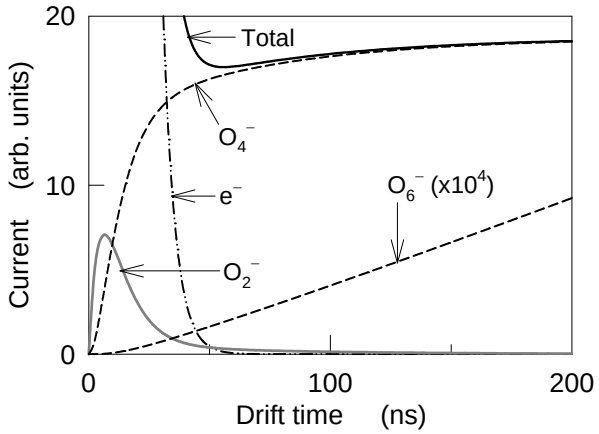

Figure 19. *Temporal evolution of the electron and ion swarms during the first 200 ns of avalanche growth/decay in O_2 [25]. The experimental conditions are the same as those in Fig. 18.*

The measured, reduced mobilities, K_0, derived from pulse shapes similar to those in Fig. 18 are plotted in Fig. 20 as a function of E/N, together with those calculated using a procedure similar to that of the negative ions of SF_6, described in Section 3.3.

The elastic momentum collision cross sections of the O_4^-/O_2 and O_6^-/O_2 systems were calculated from a JWKB approximation, while the inelastic cross sections were taken from the literature [25]. These sets of collision cross sections were validated from an optimised Monte Carlo algorithm, using the measured mobility data.

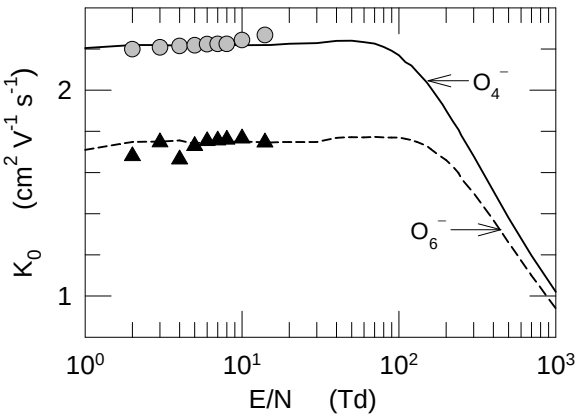

Figure 20. *The mobility of O_4^- and O_6^- in SF_6. Symbols: measurements; solid and broken curves: calculations [25].*

The collision cross section sets are shown in Fig. 21 for O_4^-/O_2 and O_6^-/O_2, respectively, as a function of the relative collision energy. The elastic momentum collision cross sections were calculated from a JWKB approximation using a (12-6-4) interaction potential. The magnitude of the elastic momentum cross section was also chosen to fit the measured (extrapolated) zero-field mobility and the other measured mobilities at low fields.

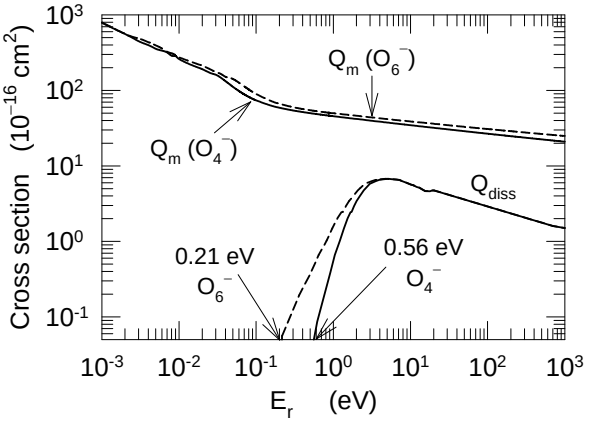

Figure 21. *Elastic momentum (Q_m) and dissociation (Q_{diss}) collision cross sections for O_4^- and O_6^- in O_2 as a function of the relative energy, and adjusted to the measurements [25].*

4. CONCLUSION

The selected examples of validation/derivation of collision cross sections of electrons and ions in gases presented in this paper are aimed at demonstrating the essential and powerful role

that a combination of swarm measurements and calculations based on Boltzmann and Monte Carlo methods play in the growing field of low temperature plasma physics and its multiple applications.

There still are many challenges ahead in the knowledge of electron and ion transport and reactivity in gases and their dependence with E/N and gas temperature. The needs are nowadays enormous in view of the growing fields of research and applications in medicine, bioplasmas, nanotechnology, new gaseous insulators, lighting and semiconductor fabrication. Further insight is needed in the study of processes such as electron detachment, Penning ionisation, ion cluster formation, light emission from excited molecules/atoms and ion interaction with walls and special deposits such as those used in plasma display panels. Fostering the connection experiment-theory even further will no doubt shed more light into this important field of fundamental and applied plasma physics.

Acknowledgements

This work was supported by Project DGAPA-UNAM IN 111611.

REFERENCES

[1] L. G. Christophorou and S. R. Hunter, *Electron Interactions in Gases and Their Applications*, Academic Press, (1984)

[2] A. Bekstein, J. de Urquijo, O. Ducasse, J. C. Rodríguez, A. M. Juárez, *J. Phys. Conf. Ser*. **370** (2012), and references therein.

[3] G. Basile, I. Gallimberti, S. Stangherlin, T.H. Teich, T H, *Proc. 20th ICPIG*, Vol. 2, p. 361 (1991)

[4] J. de Urquijo, A.M. Juárez, E. Basurto, J.L.Hernández-Ávila, *Eur. Phys. J. D* **51**, 241 (2009)

[5] O. Šašić, S. Dupljanin, J.de Urquijo and Z. Lj. Petrović, *J. Phys D* **46** 325201 (2013)

[6] S. Biagi, *Personal communication*, http://rjd.web.cern.ch/rjd/cgi-bin /cross?update (2007)

[7] O. Šašić, J. de Urquijo, A.M. Juárez, S. Dupljanin, J. Jovanović, J.L. Hernández-Ávila, E. Basurto, and Z. Lj. Petrović, *Plasma Sources Science and Technology* **19** 034003 (2010)

[8] Z Lj Petrovic, T.F. O'Malley, R.W. Crompton, *J. Phys.B: At. Mol. Opt. Phys.* **28** 3309 (1995)

[9] Z Lj Petrovic and R.W. Crompton R *Aust. J Phys.* **40** 347 (1987)

[10] R.W. Crompton *Adv. At. Mol. Opt. Phys.* **32** 97 (1994)

[11] L.G.H. Huxley and R.W. Crompton, *The Diffusion and Drift of Electrons in Gases,* New York: Wiley-Interscience (1974)

[12] J. L. Hernández-Ávila, E. Basurto, J. de Urquijo, *J. Phys. D*, **35** 2264 (2002)

[13] Y. Itikawa and N. Mason, *J. Phys. Chem. Ref. Data*, **34** 1 (2005)

[14] K. F. Ness, R. E. Robson, M. J. Brunger, R. D. White, *J. Chem. Phys.* **136** 024318 (2012)

[15] B. Cheung and M. T. Elford, *Aust. J. Phys*. **43**, 755 (1990).

[16] H. Hasegawa, H. Date, and M. Shimozuma, *J. Phys. D* **40**, 2495 (2007).

[17] G. Ruiz-Vargas, M. Yousfi, and J. de Urquijo, *J. Phys. D* **43**, 455201 (2010).

[18] K. F. Ness and R. E. Robson, *Phys. Rev. A* **38**, 1446 (1988).

[19] M. Yousfi and M. D. Benabdessadok, *J. Appl. Phys.* **80**, 6619 (1996).

[20] S. Dupljanin, J. de Urquijo, O. Šašić, E. Basurto, A.M. Juárez, J.L. Hernández Ávila, S. Dujko and Z. Lj. Petrović, *Plasma Sources Science and Technology* **19** (2010) 025005

[21] D. Piscitelli, A.V. Phelps, J. de Urquijo J, E. Basurto, L.C. Pitchford, *Phys. Rev. E* **68**, 046408 (2003)

[22] J. de Urquijo, E. Basurto and A. Bekstein, J. Phys. D **44** 325202 (2011)

[23] J. de Urquijo, J.V. Jovanović, A. Bekstein, V. Stojanović, Z.Lj. Petrović, *Plasma Sources Science and Technology* **22** 025004 (2013)

[24] M. Benhenni, M. Yousfi, J. de Urquijo and A. Hennad, *J. Phys. D* **42** 125203 (2009)

[25] J. de Urquijo, A. Bekstein, O. Ducasse, G. Ruíz-Vargas, M. Yousfi, M. Benhenni, Eur. Phys. J. D, **55** 637 (2009)